Activation Mechanism of Corticotrophin Releasing Factor Receptor Type 1 Elucidated Using Molecular Dynamics Simulation

Abdullahi Ibrahim Uba^{1a}, Nicolas Scorese^{2a}, Emily Dean², Haiguang Liu^{1*} and Chun Wu^{2*}

¹Complex Systems Division, Beijing Computational Science Research Center, Beijing 100193, China

a: Both authors contributed equally to this work

² College of Science and Mathematics, Rowan University, Glassboro, NJ, 08028 USA

^{*} To whom correspondence should be addressed: Chun Wu: wuc@rowan.edu; Haiguang Liu: hgliu@csrc.ac.cn

Abstract

The corticotropin-releasing factor receptor type 1 (CRF1R), a member of Class B G-proteincoupled receptors (GPCRs), is a good drug target for treating depression, anxiety, and other stress-related neuro-disorders. However, there is no approved drug targeting the CRF1R to date, partly due to inadequate structural information and its elusive activation mechanism. Here, using the crystal structures of its transmembrane domain (TMD) and the N-terminal extracellular domain (ECD) as a template, a full-length homology model of CRF1R was built and its complexes with peptide agonist Urocortin 1 and small molecule antagonist CP-376395 were subjected to all-atom molecular dynamics simulations. We observed relative rigid helices with helical contents well preserved through simulations, while the transmembrane helices (TMs) showed rearrangements, in particular the TM6 in the agonist-bound CRF1R. The observed conformational changes are likely due to breakage of inter-helical/inter-regional hydrogen bonds in the TMD. Dynamical network analysis identifies communities with frequent connections to TM6. Three key residues, Y356^{6.53}, Q384^{7.49}, and L395^{7.60}, identified from the simulation and network analysis corroborate with experimental mutagenesis data, indicating their important roles in the activation of the receptor. The observed large-scale conformational changes and the underlying mechanism are related to CRF1R activation by agonist binding, providing guidance for ligand design.

Keyword: corticotropin-releasing factor receptor type 1, Urocortin 1, molecular dynamics simulation, dynamical network analysis, activation mechanism

Introduction

G-protein-coupled-receptors (GPCRs) are the largest family of cell surface receptors in human genome sharing the same topology, which comprises seven transmembrane (7TM) helices connected by alternating intracellular and extracellular loops, an extracellular N-terminus, and an intracellular C-terminus. GPCRs possess a tremendous therapeutic potential, and over 40% of the approved drugs target GPCRs. They can be grouped into five distinct classes based on sequence homology and functional similarity: Class A (rhodopsin), Class B (secretin), Class C (glutamate), Class D (adhesion), and Class E (frizzled) ¹. Class A, containing over 700 receptors, are the largest GPCR class that is best studied from the wealth of structural information on these receptors, which greatly increases molecular understanding of functions and activation mechanism²⁻⁵. Class B GPCRs are distinguished by their large cysteine-rich extracellular domain which plays an important role in activation and there are 15 known receptors in this family that are implicated in stress- and anxiety-related neuro-disorders, diabetes, osteoporosis, hypercalcemia^{6, 7}. However, unlike Class A receptors, limited knowledge is available about the activation mechanism of Class B GPCRs (the second largest class) beyond a general binding mechanism for peptide hormones 8-10.

The corticotropin-releasing factor receptor type 1 (CRF1R) is a Class B GPCR predominantly found in the central nervous system, involved in the regulation of adenocorticotropic hormone (ACTH), a key modulator in stress response ¹¹. Thus, CRF1R is a good drug target for anxiety, depression, inflammation, and other stress related neuro-disorders ¹². The activation mechanism remains largely unknown due to the limited availability of class B GPCR structure. Class B natural agonists turn into partial agonists and then into antagonists by successively truncating residues at the N-terminus ^{13, 14}. Seidal et al. ⁸ investigated the molecular mechanism of this

phenomenon using flexible peptide docking and conformational sampling of the full-length Rat CRF1R complexed with Corticotropin-releasing factor (CRF) and peptide antagonists derived by N-truncation of peptide agonists CRF and Urocortin 1. In their study, the molecular interaction was guided by experimentally derived pair-wise crosslinking restraints. They found that the peptide antagonists stabilize different conformations of the transmembrane domain (TMD) of CRF1R in respect to the agonists. While preserving inter-residue contacts, both the agonist- and the antagonist-bound models show substantial flexibility throughout the simulations. However, the detailed conformational changes involving specific structural units and their possible communication patterns have not been addressed.

The C-terminal of the peptide hormone non-covalently attaches to the N-terminal extracellular domain (ECD) of the CRF1R receptor, initiating a conformational change that allows the N-terminal of the peptide to bind inside the seven transmembrane pocket. This conformational change affects the interaction with the G protein ¹⁵. In contrast, small-molecule antagonists, such as CP-376395, act allosterically within the TMD to inhibit the binding of the peptide-agonist ligands. To get insights into the antagonist binding, Xu et al. ¹⁶ studied the dynamics of CRF1R in complex with CP-376395 and MTIP, compared to an apo form of the receptor. Xu and coworkers found that the "ionic lock" between side chains of R151^{2,46} in TM2 and E209^{3,50} in TM3 (the numbering is based on the crystal structure of Rat CRF1R (PDB ID: 4K5Y)) is broken in apo-CRF1R, but it is stabilized in the antagonist-bound CRF1Rs. However, the MD simulations in that study were only 100 ns, not sufficiently long to observe conformational changes that occur at longer time scales ¹⁶.

Here, we provide more insights on CRF1R activation mechanisms by extensively sampling conformations via all-atom molecular dynamics (MD) simulations. Using homology modeling,

we built the full-length structure of human CRF1R based on the available structures of TMD (PDB ID: 4K5Y)¹⁷ and the N-terminal ECD (PDB ID: 3EHU) ¹⁸ of the Rat CRF1R. The peptide agonist Urocortin 1 was inserted into the CRF1R model in accordance with a previous study 9, while the co-crystallized ligand in 4K5Y, the antagonist CP-376395, was transferred to its orthosteric binding site of the CRF1R structure. Three independent 1000-ns MD simulations with different initial velocities were performed for each system. We observed large-scale conformational changes at the N-terminal ECD which triggers the movement of TM6, opening the transmission switch (located between TM6 and TM7) in the agonist Urocortin 1-bound CRF1R. On the other hand, the antagonist CP-376395-bound CRF1R appears to maintain the initial inactive conformation. Furthermore, CRF1R-ligand interaction analysis and dynamical network analysis revealed key interacting residues and critical residues, which are crossvalidated with the experimental mutagenesis data in literature. Based on the discoveries, we propose a signal transduction path from the ligand binding site to transmission switch site. Simulations reveal that agonist-induced conformational changes are essential for CRF1R activation, providing insights that may aid drug design targeting this receptor.

Results

Urocortin 1 inserts into a groove between TM5 and TM6

The full-length homology model of CR1FR comprises the N-terminal ECD, TMD, and C-terminal helix 8. The N-terminal ECD is connected to the TMD via a flexible linker (Supplementary Figure S1). In the complex structure, the Urocortin 1 C-terminus interacts with the N-terminal region of the receptor, and the N-terminus of the peptide interacts with the TMD at the groove between TM5 and TM6 (Figure 1A). The antagonist CP-376395 transferred from

the crystal structure (PDB ID 4KBY) to the full-length CRF1R homology model sits deep in the pocket (Figure 1B).

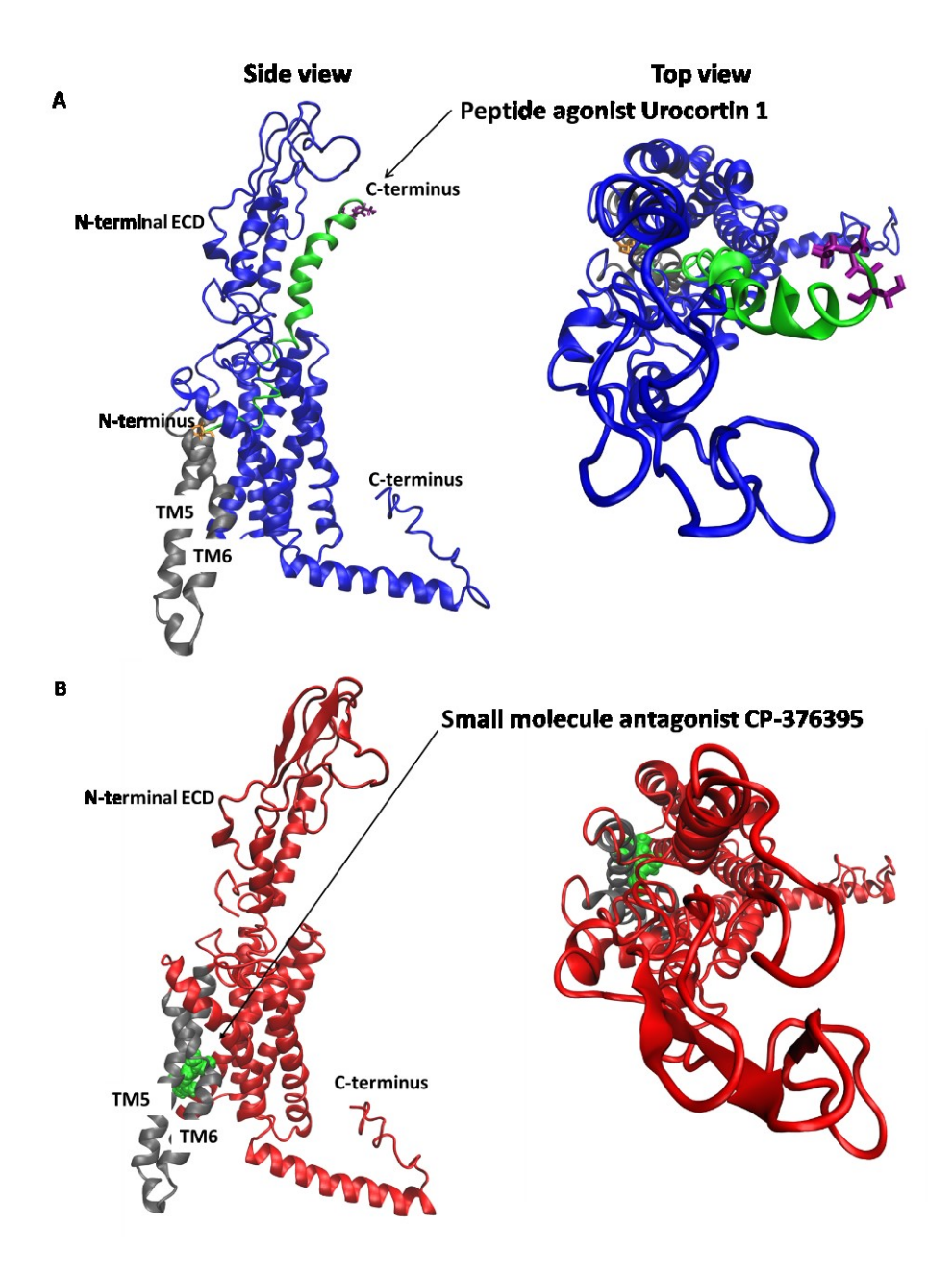


Figure 1. Initial models of CRF1R with ligands. (A) Binding pose of the peptide agonist Urocortin 1 (green colored cartoon representation). (B) Binding pose of small molecule antagonist CP-376395 (in the van der Waals representation, colored in green). The side and top views are shown on the left and right panels, respectively.

Large Conformational Change is observed in the agonist-CRF1R

After aligning structures sampled in simulations to the TMD of initial model, Root-Mean-Square-Deviation (RMSD) values for sub-regions of CRF1R receptor reveal pronounced movements occurring to TM6 in the agonist bound system. This is verified by a clear reduction in RMSD values after excluding TM6 from the alignment (Supplementary Figures S2-S4). The N-terminal ECD of the Urocortin1-bound CRF1R undergoes a major conformational change to reach a stable state at around 300 ns. The changes in ECD are correlated to structural changes of the TMD as well as to the movement of TM6 (Figure 2A). The antagonist CP-376395-bound CRF1R appears to maintain the inactive conformation of the TMD and shows relatively smaller structural changes at the N-terminal ECD, although C-terminal regions (helix-8) of CRF1R appears to have larger structural changes (Figure 2B). The average RMSD values computed for the last 500 ns of the specific regions of the CRF1R are compared in Table 1 for the systems with agonist or antagonist ligands. The progression of conformational changes of CRF1R are summarized by superimposing conformations at four time points to the initial model of CRF1R for both agonist and antagonist bound systems (Figures S5-6). Large movement of the Nterminal ECD were observed in two of out three trajectories of the agonist-bound system. In the case of the antagonist-bound system, smaller deviation of the N-terminal ECD, larger deviation of the C-terminal region and subsequent loss of helical structure are observed.

The $C\alpha$ Root-Mean Square Fluctuation (RMSF) analysis show consistent patterns with the structural deviation results revealed in the RMSD plots, with the N-terminal ECD and C-terminal regions exhibit larger fluctuations in both systems (see Figure S7, and a tabulated summary in Table S1 for regional averaged RMSF values). The TMD (especially TM1, 5, 7) and extracellular loops (ECLs) 2 and 3 show slightly higher fluctuations in the agonist-bound system

than in the antagonist-bound system. This agrees with the study by Seidel et al.⁸ that both agonist and antagonist systems maintain integrity and flexibility during simulation, and that the ECL3 shows higher fluctuations than other loops.

Table 1. Average values of RMSD in sub-regions of the agonist Urocortin 1-bound and antagonist CP-376395-bound CRF1Rs. The RMSD are calculated between initial structure and the structures of the last 500 ns simulations, after aligning to TMD (without TM6).

ъ.	Agonist-CRF1R	Antagonist-CRF1R		
Region	Cα RMSD (Å)	Cα RMSD (Å)		
N-terminal ECD	17.2 ± 0.3	8.2 ± 0.2		
TMD	4.5 ± 0.2	2.7 ± 0.2		
TM6	8.1 ± 0.2	5.2 ± 0.7		
C-terminal	4.4 ± 0.2	7.2 ± 0.4		
Ligand	3.2 ± 0.8	3.5 ± 0.3		

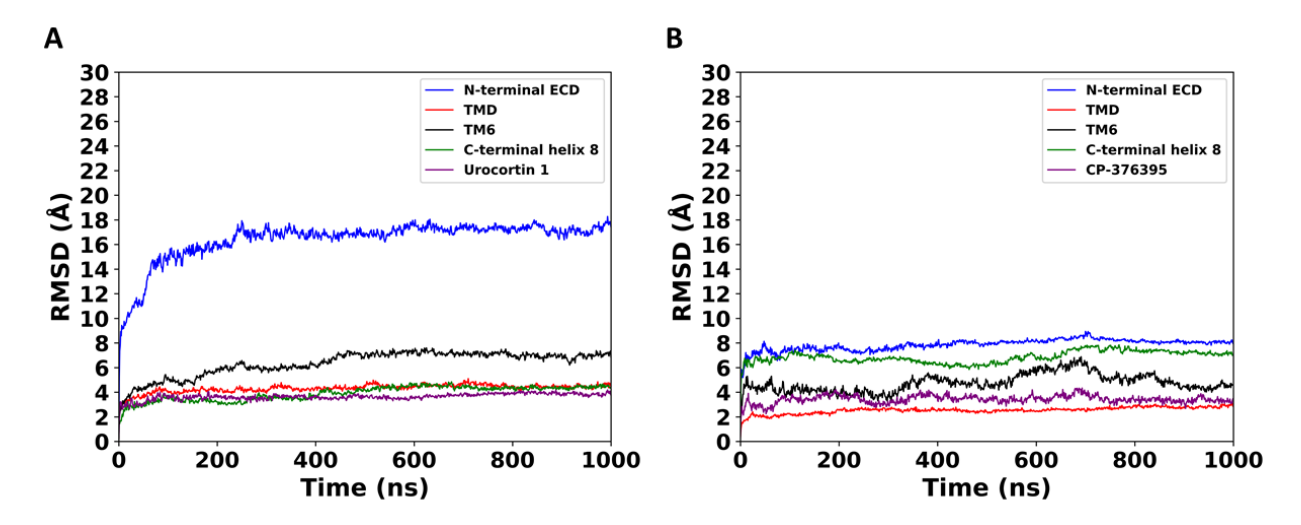


Figure 2. The Cα Root Mean-Square Deviation (RMSD) profiles (averaged over 3 trajectories) of the sub-regions for (A) agonist Urocortin 1-bound CRF1R and (B) antagonist CP-376395-bound CRF1R. All structures were aligned to the transmembrane helices TM1-5 and TM7 of the initial model.

The agonist Urocortin1 and the antagonist CP-376395 form different interactions with CRF1R

The interactions between CRF1R and ligands for the most abundant structure are presented in Figure 3. The agonist Urocortin1 forms several contacts with the N-terminal ECD and a few contacts with the TMD (Figure 3A and B). The first 8 residues of Urocortin 1 interacts with the TMD, whereas residues 9-41 form contacts with the N-terminal ECD of the CRF1R. The persistent contacts (observed in more than 20% of simulation time) reveal detailed interaction patterns. The strongest interaction is a salt bridge between K291^{ECL2} in CRF1R and D2 in Urocortin 1 (Figure 3C). The stable CRF1R-Urocortin1 interactions (with over 10% occupancy through simulations) comprising H-bonds, salt bridges, and phi-cation interactions, are shown in the snake representations of the CRF1R and Urocortin 1 (Figure S8A and B). The corresponding interaction between the antagonist CP-376395 and CRF1R is presented in Figure S8C. The

antagonist CP-376395 binds to the CRF1R via both hydrophobic interactions and hydrogen bonding interactions (Figure 3D-F). The detailed interactions between CRF1R and Urocortin 1 are shown in two dimensions (2D) diagram (Figure S9). Among the key interacting residues of CRF1R (>10% of the simulation time), 14 residues at the ECD, TM2, ECL1, ECL2, and ECL3 are found to overlap with the mutagenesis data (Figure S10). The CRF1R residue K291^{ECL2} and the D2 of Urocortin 1 form the most persistent interaction (>80% through the simulations) which is consistent with in vitro mutation data.

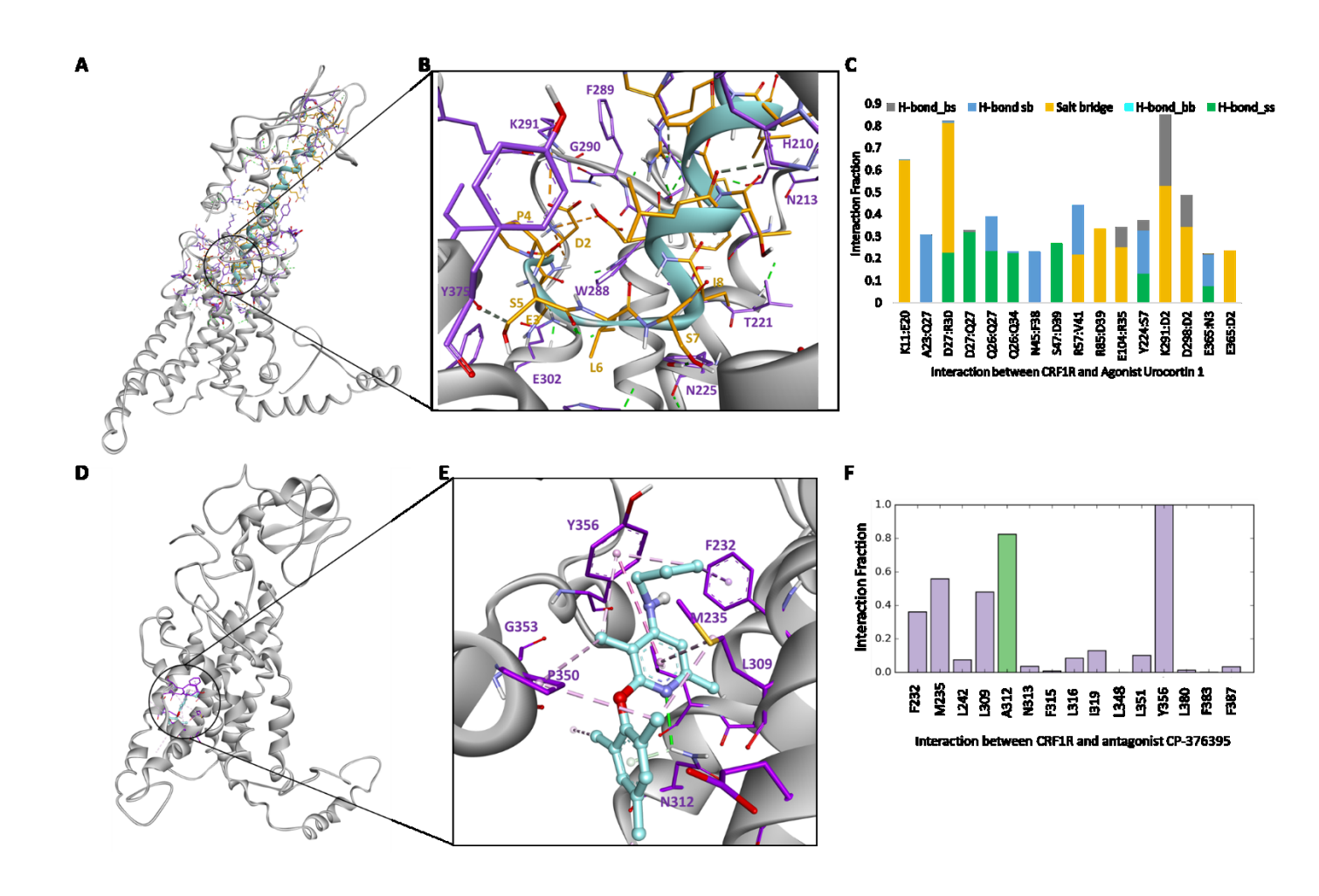


Figure 3. Interactions between CRF1R and ligands. (A) The overview of interactions in the agonist-bound system for the most abundant structure. (B) Detailed interactions between the N-terminal residues of Urocortin 1 and the TMD of CRF1R. The interacting residues are shown in licorice representation (CRF1R: purple; Urocortin 1: Orange). (C) Persistent interaction (in more than 20% of the simulations) between agonist Urocortin 1 and CRF1R. (D and E) Interaction for the antagonist-bound system. (F) Composition of interactions between CRF1R and antagonist CP-376395. The interactions are color coded as the following: H-bond_ss (side chains-side) (green), H-bond_sb (side chain-backbone) (blue), and H-bond_bs (backbone-side chain) (gray), salt bridge (yellow), and hydrophobic interaction (pink).

Stabilization of secondary structure in the agonist-bound CRF1R

The agonist Urocortin 1-bound CRF1R maintains helical content despite rearrangement of the TM helices (Figure 4A). On the other hand, the helical content of the antagonist CP-356395-bound CRF1R lost helical structure (Figure 4B). The average of the helices over all residues are about 56% for the agonist system and 31% for the antagonist system.

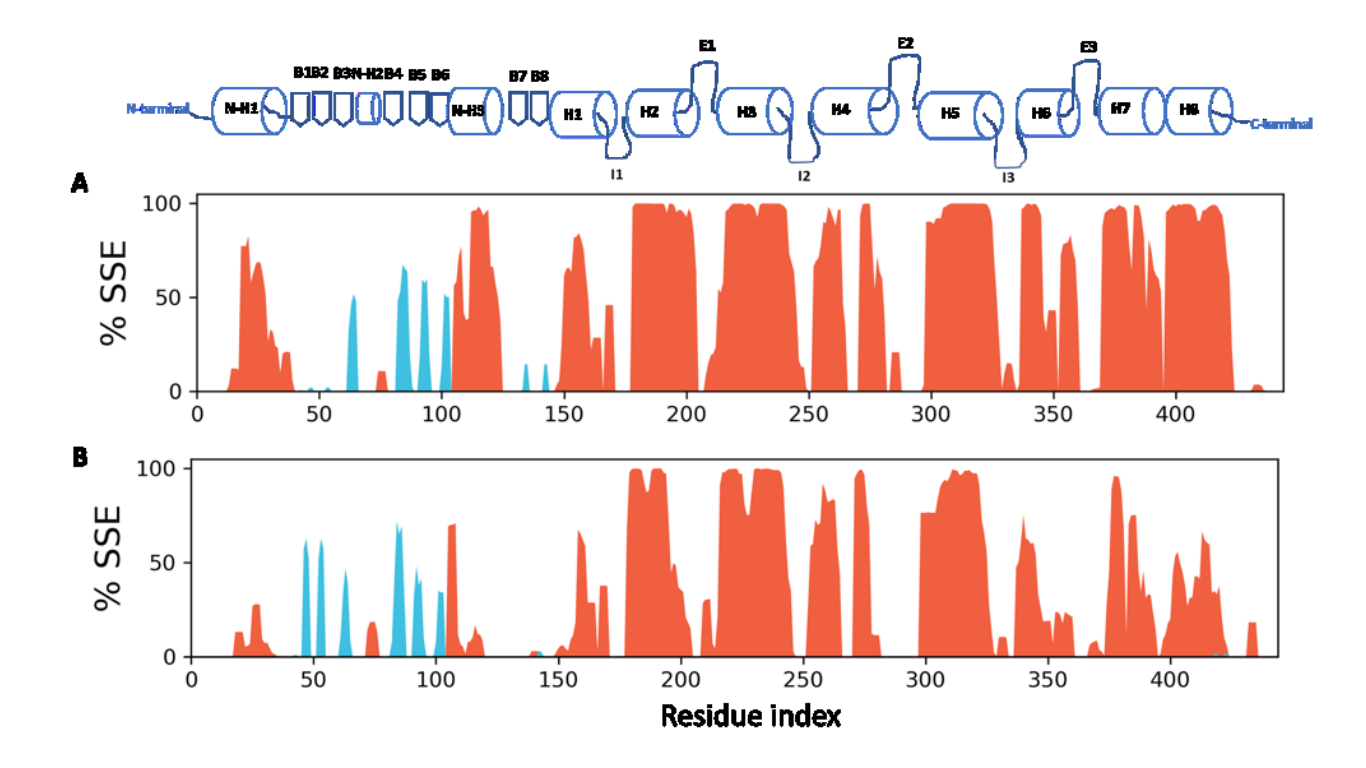


Figure 4. Secondary structure elements. (**A**) agonist-bound CRF1R. (**B**) antagonist-bound CRF1R. Orange represents alpha helices; blue represents beta sheets. N-terminal region: residues

0-145, TM1: 146-170, TM2: 178-205, TM3: 215-248, TM4: 255-281, TM5: 298-330, TM6: 333-361, TM7: 370-395, C-terminal region: 396-444.

Activated structure of agonist bound CRF1R revealed by structure comparison

Clustering analysis based on Cα-RMSD between conformations grouped agonist-bound CRF1R into 6 clusters, and antagonist-bound CRF1R into 10 clusters, both with 2.5 Å RMSD as cutoff distance. Representative structures of clusters accounting for ≥ 5% of total population are shown in Figure S11. The most abundant clusters represent 34% for the agonist-bound CRF1R and 29% for the antagonist-bound CRF1R, and their representative structures are compared in detail (Figures 5 & 6). Two key differences are observed around the TMD region: (I) Increase in the distance between TM6 and TM7 compared to the initial model, caused by the bending of TM6 towards TM5 in the agonist system. In case of the antagonist CP-356395-bound CRF1R, the C-terminal helix 8 bends downward, pushing the end of TM7 inward thereby shortening the distance between the two transmembrane helices. (II) Shifting of TM1, 5-7, likely caused by the interaction between Urocortin 1 and residues in the groove between TM5 and TM6. The conformational differences for TM2, TM3, and TM4 are small between the two systems.

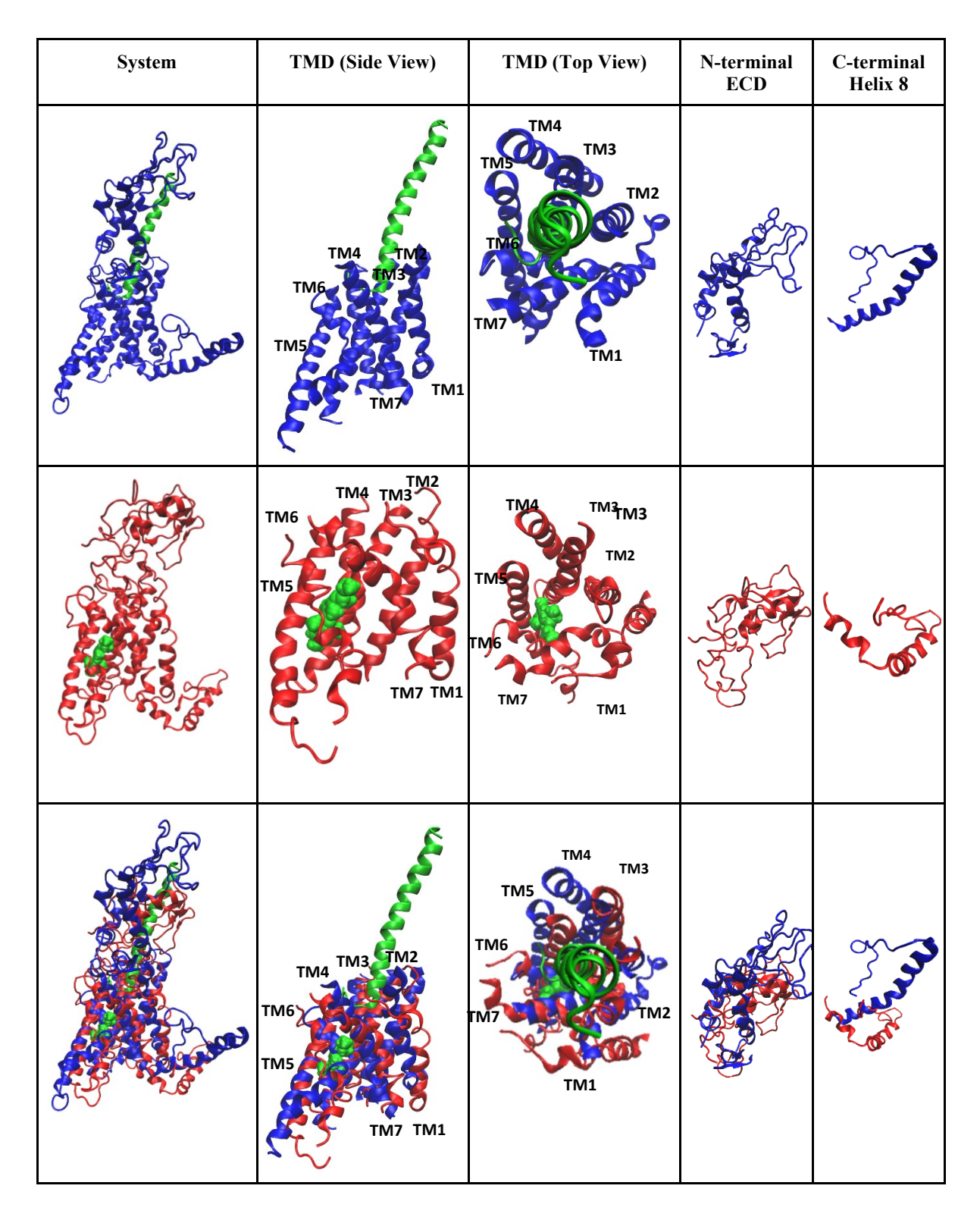


Figure 5. Comparison of representative structures for the most abundant clusters. Blue color: agonist Urocortin 1-bound CRF1R (34%); Red color: antagonist CP-376395-bound CRF1R system (29%); Green color: ligands.

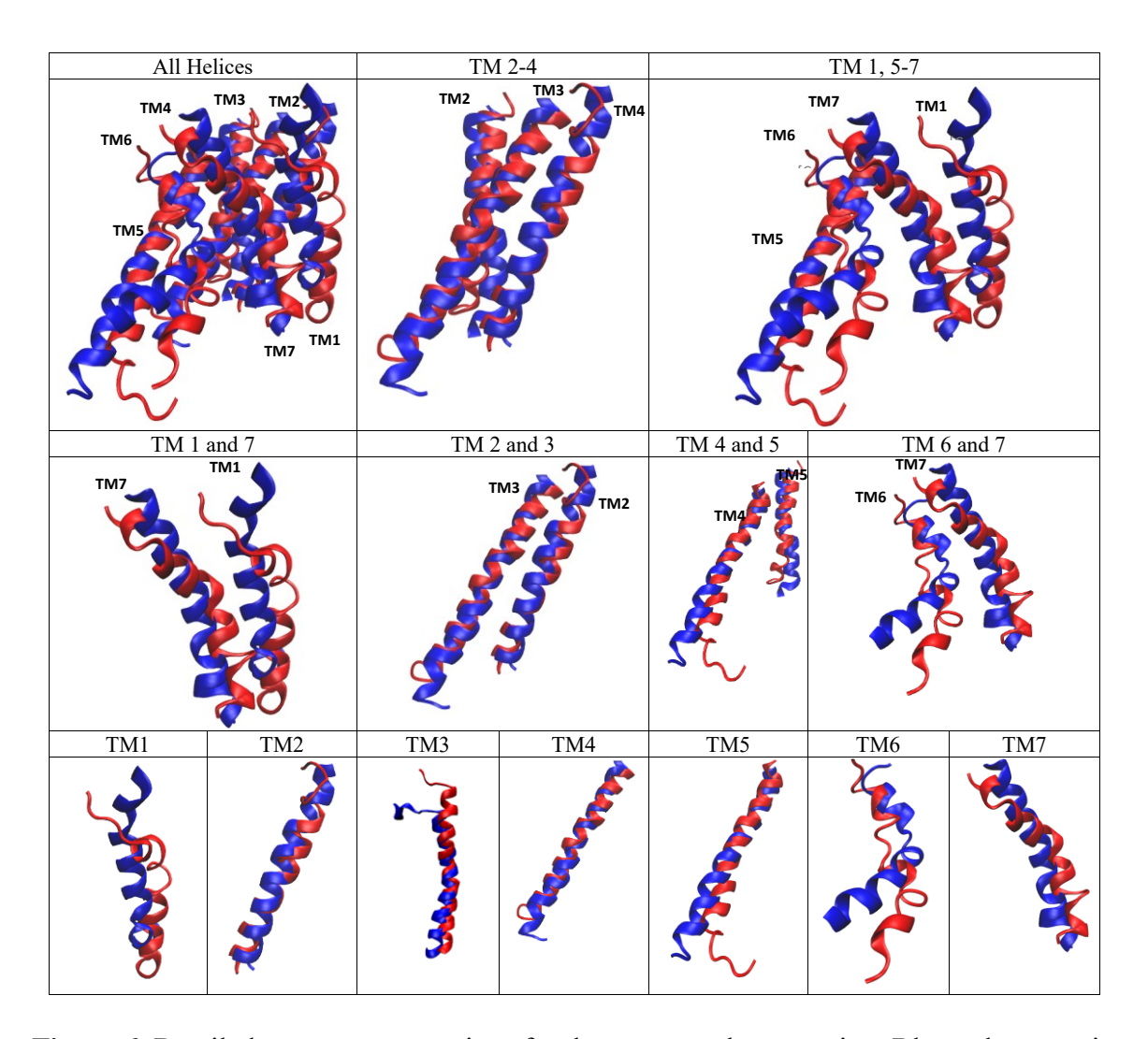


Figure 6. Detailed structure comparison for the transmembrane region. Blue color: agonist Urocortin 1-bound CRF1R; Red color: antagonist CP-376395-bound CRF1R. TM1, 5-7 show high deviation in the agonist Urocortin 1-bound CRF1R, whereas TM2, 3 and 4 retain their position in both systems.

Possible active conformation for the agonist-bound CRF1R

The common hallmark of class-B GPCRs activation is their ability to adopt a conserved conformation for G-protein docking. Therefore, the agonist Urocortin 1-bound CRF1R and antagonist CP-376395-bound CRF1R were superimposed on GLP1R (another member of class-B GPCRs) based on their TMD. The C-terminal region of the agonist system adopts similar conformation to that of the GPL1R. Helix 8 is slightly tilted upward pulling TM7, opening the

space between TM6 and TM7 for the G-protein to dock. However, a few clashes may occur which requires structure optimization (Figure 7A). In the case of the antagonist CP-376395-bound CRF1R, the C-terminal uncoils and angles further downward pushing TM7 toward TM6 and thereby narrowing the G-protein binding site. This alignment reveals clashes around the intracellular loop 3 (IL3) and helix 8 which are both pulled inward, likely due the binding of the antagonist CP-376395 in the pocket (Figure 7B).

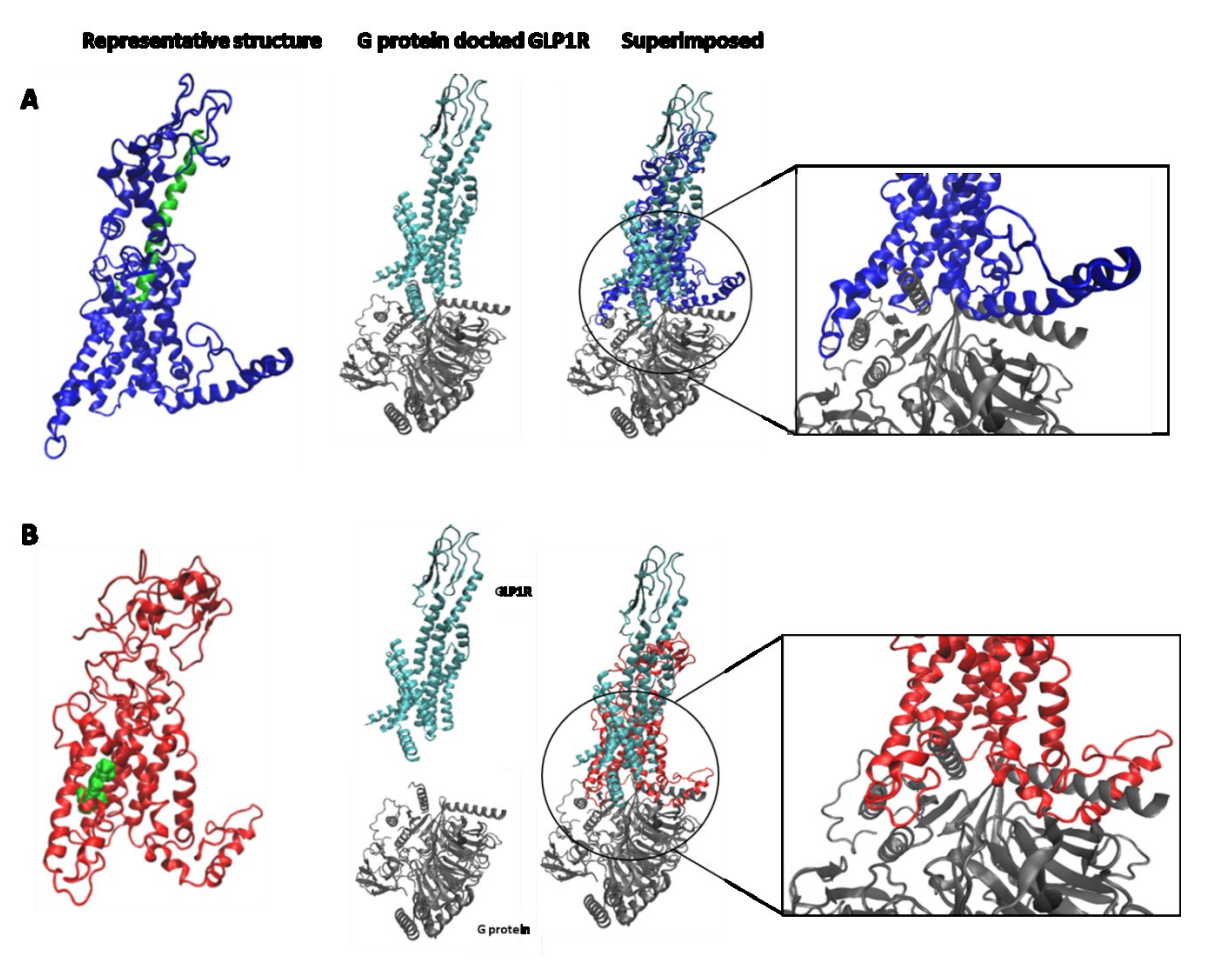


Figure 7. Comparison of the representative structure of the most abundant clusters. **(A)** Agonist Urocortin 1-bound CRF1R. **(B)** Antagonist CP 376395-bound CRF1R superimposed on the Glucagon-like peptide-receptor 1 (GLP1R). The Agonist Urocortin 1-bound CRF1R adopts a potentially active conformation that may allow for G-protein binding.

Residue distance analysis suggest activation in the agonist-bound CRF1R

Molecular switches are a set of non-covalent interactions whose disruption causes the GPCRs to enter an activated state ¹⁹. Unlike in class A GPCRs, canonical motifs for these microswitches in the class B GPCRs are still unknown. In search for such motifs, potential molecular switches examined by previous studies ^{16, 20} were analyzed in this study: ionic lock between R180^{2.46} and E238^{3.50}; and polar lock between H184^{2.50} and E238^{3.50}. In addition, we analyzed the residue distance between S333^{6.30} and L395^{7.59}, several inter-helical/inter-regional salt bridges, and hydrogen bonds (Table S5). Together, we analyzed 21 distances between residues to reveal the dynamics during CRF1R activation and found nine distances exhibit increasing trends in the agonist-bound CRF1R (Table 2). The residue distance between S333^{6.30} and L395^{7.59} increases from 18.4 Å to 28.20 Å in the agonist Urocortin 1-bound CRF1R, while it decreases to 14.75 Å in the antagonist CP-376395-bound CRF1R (Figure 8C). The timelines for these 3 distances are shown in Figure 8A, where a general increasing trend is observed in the agonist Urocortin 1bound CRF1R. In the representative structures shown in Figure 8A, the R180^{2.46}:E238^{3.50} ionic lock is broken in the agonist Urocortin 1-bound CRF1R, while it remains intact in the antagonist CP-376395-bound CRF1R. This is consistent with the results of Xu et al. ¹⁶ that ionic lock is broken in apo CRF1R structure, presumably due to the intrinsic activity of the receptor. Another salt bridge between K291^{ECL2} and D298^{5.60}, close to the peptide binding site, is broken in the Urocortin 1-bound CRF1R, but it is intact in the CP-376395-bound CRF1R (Figure 8B)The timeline of all 21 distances examined are presented in Figure S12, with mean distances summarized in Table S3.

Table 2. Distances between residues (averaged over 3 trajectories) with increasing trends in agonist bound system. The change relative to the initial model for last 100 ns: increased distance (blue); decreased distance (red).

		Agonist Urocortin 1-bound CRF1R			Antagonist CP-376395-bound CRF1R		
Index No	Distance (Å)	1000 ns	First 100 ns	Last 100 ns	1000 ns	First 100 ns	Last 100 ns
1	R180 ^{2.46} :E238 ^{3.50}	6.9 ± 0.4	7.5 ± 0.9	6.7 ± 0.3	3.3 ± 0.9	5.4 ± 0.9	2.6 ±0.6
3	S333 ^{6.30} :L395 ^{7.60}	19.3 ± 1.8	17.3 ± 1.3	20.8 ± 2.9	16.7 ± 1.2	17.1 ± 0.4	17.2 ± 0.2
7	R180 ^{2.46} :E398 ^{H8}	11.9 ± 0.7	8.4 ± 1.4	13.3 ± 0.7	3.9 ± 0.4	4.2 ± 0.6	3.8 ± 0.8
8	D156 ^{1.76} :R194 ^{2.60}	12.8 ± 2.3	3.7 ± 1.2	14.2 ± 0.6	4.5 ± 0.6	3.6 ± 0.5	5.4 ± 0.9
9	D283 ^{4.68} :R292 ^{ECL2}	6.1 ± 1.0	5.8 ± 0.6	8.2 ± 0.8	3.5 ± 0.4	4.1 ± 0.9	3.4 ± 0.5
10	E285 ^{ECL2} :R292 ^{ECL2}	8.6 ± 1.3	7.8 ± 1.1	12.5 ± 1.3	5.0 ± 0.4	4.6 ± 0.8	5.7 ± 0.6
11	K291 ^{ECL2} :D298 ^{5.36}	7.35 ± 1.23	7.3 ± 0.9	11.8 ± 3.1	5.3 ± 0.6	6.6 ± 1.0	4.3 ± 0.7
19	E160 ^{1.76} :N195 ^{2.61}	6.2 ± 0.5	5.8 ± 1.2	5.8 ± 0.8	4.2 ± 0.3	4.5 ± 0.6	3.9 ± 0.3
20	Y356 ^{6.53} :Q384 ^{7.49}	11.1 ± 0.7	9.5 ± 2.2	10.5 ± 1.0	4.8 ± 0.3	5.2 ± 0.6	4.8 ± 0.4

Note: Distances 1 and 7-17 were measured between O and N; Distance 3 was measured between Center of Mass of S333^{6,30} and L395^{7,60}. Distances 18 to 21 were measured between NH and O and between OH and N. N312^{5,50} 86% conserved in class B and subfamily B1 of class B GPCRs. R180^{2,46}, H184^{2,50}, E238^{3,50} and Q384^{7,49} are 83% conserved in class B and subfamily B1 of class B GPCRs. R194^{2,60}, Y356^{6,53}, and E398^{H8} are 66%, 72%, and 83% conserved, respectively, in subfamily B1 of class B GPCRs. Y356^{6,53}, Q384^{7,49}, and L395^{7,60} are critical residues identified by network analysis that overlap with mutagenesis data. K291^{ECL2} is a key interacting residue (Occupancy: >80%) that overlap with mutagenesis data. The complete 21 distances examined are presented in the supplementary Table S2.

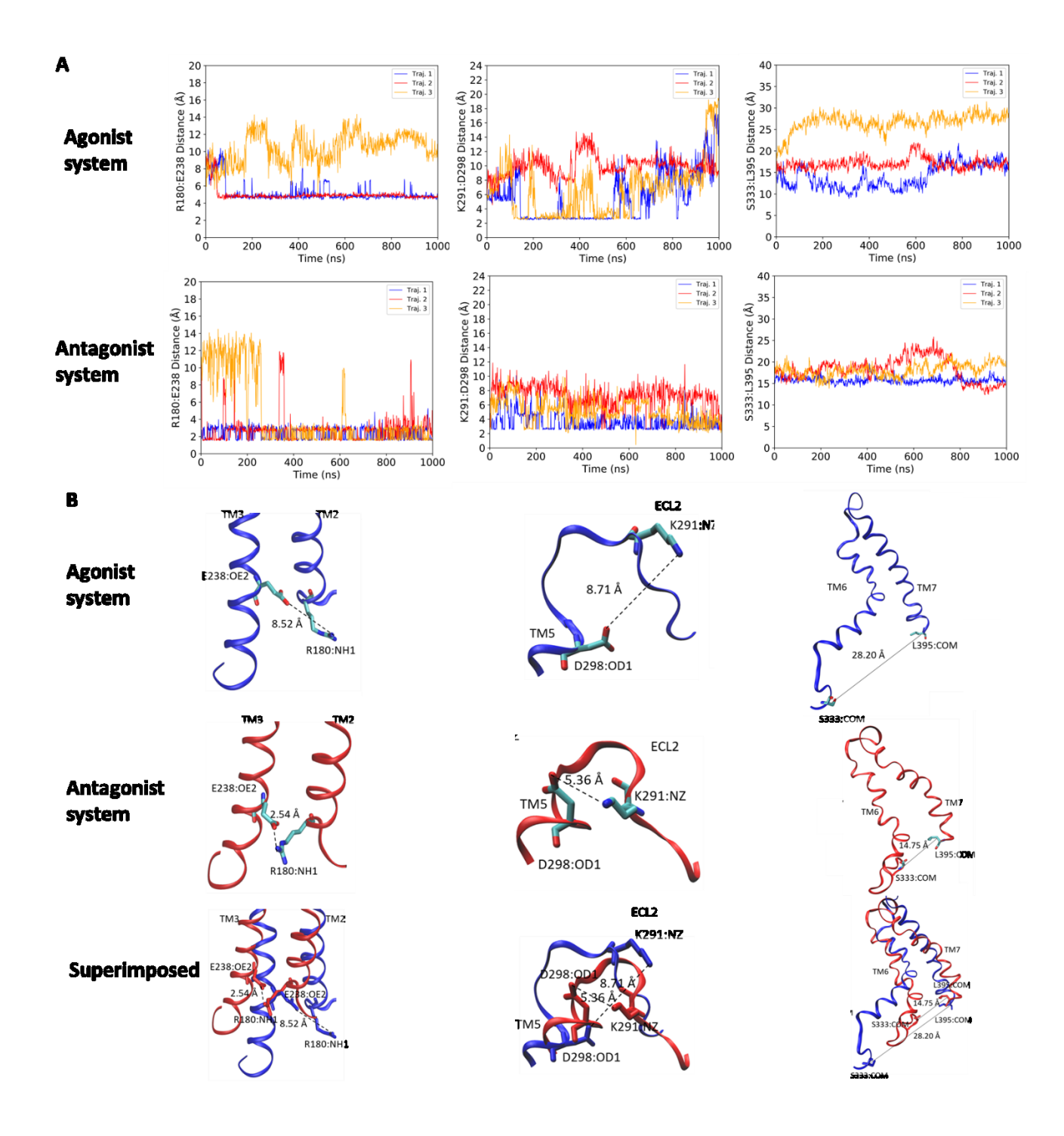


Figure 8. Timeline for molecular switch residue distance. Ionic lock between R180^{2.46} and E238^{3.50} (**Distance 1**); a potential salt bridge between K291^{ECL2} and D298^{5.36} (**Distance 11**); and gate residue distance (Center of Mass) between S333^{6.30} and L395^{7.59} (**Distance 3**). The salt bridges appear to be broken over time in the agonist Urocortin 1-bound CRF1R while stabilized in the antagonist CP-376395-bound CRF1R. The Center of Mass residue distance of the transmission switch gate residue shows increasing trend in the agonist Urocortin 1-bound CRF1R compared with the antagonist CP-376395-bound CRF1R.

(B) Comparison of molecular switch residue distance for the representative of the most abundant cluster of the agonist Urocortin 1-bound CRF1R (Blue) and antagonist-bound CRF1R (Red). Ionic lock between R180^{2.46} and E238^{3.50} (**Distance 1**); a potential salt bridge between K291^{ECL2} and D298^{5.60} (**Distance 11**); and gate residue distance (Center of Mass) between TM6 S333^{6.30} and L395^{7.59} (**Distance 3**).

Dynamical network analysis reveals critical nodes and a possible signal transduction path

Dynamical network model was used to identify protein structural units (referred to as communities) exhibiting correlated movements, pathways for allosteric activation, as well as critical residues ²¹. A comparison of the models between the agonist and antagonist systems is presented in Figure 9. Weighted network representations were generated, with the thickness of edges between communities reflecting their correlations. Stronger correlations are observed at Nterminal ECD, peptide-TMD interaction site in the Agonist Urocortin 1-bound CRF1R (Figure 10A). In contrast, antagonist CP-376395-bound CRF1R has strongly correlated regions at the Cterminal (Figure 9B). Eighteen communities in the agonist Urocortin 1-bound CRF1R and 16 communities in the antagonist CP-376395-bound CRF1R are depicted in different colors and critical residues connecting communities were highlighted for both systems (Figure 9A,B). A path of communication from the ligand binding sites to TM6 was generated for each system. For the agonist Urocortin 1-bound CRF1R, K291^{ECL2} salt bridged to D2 of the Urocortin 1 was chosen as the starting node (signal source), and V361^{6.58} the last residue on TM6, was used as the ending node (sink). An optimal path of communication involving 8 relaying residues on TM5 and TM6 was generated (Figure 9A). For the antagonist CP-376395-bound CRF1R, N312^{5.50} that forms stable H-bond with the CP-376395 was considered as the source, relaying signal to Val361^{6.58} via a pathway shown in Figure 9B. Also, the unweighted networks and communities show similar features as the weighted ones, providing more information about the connection

between different structural units. In addition to the possible signal transduction path, alternative means of communication—referred to as suboptimal paths, were generated (Figure S13).

Critical residues from the network analysis were cross-referenced with experimental mutagenesis data (Figure S14A and B) obtained from the GPCR database (https://gpcrdb.org/). For the antagonist CP-376395-bound CRF1R, 3 out of 39 critical residues are found to overlap with mutagenesis data. The mutation data include natural genetic variation and in vitro mutants that affect binding/potency. Among the critical residues in agonist Urocortin 1-bound CRF1R, 7 residues overlap with the conserved residues in class B (Figure S15), and 11 residues overlap with the conserved residues in subfamily B1 (Figure S16, Table S4). The locations of the overlapping residues are also shown in the snake plot representation of CRF1R (Figure S17).

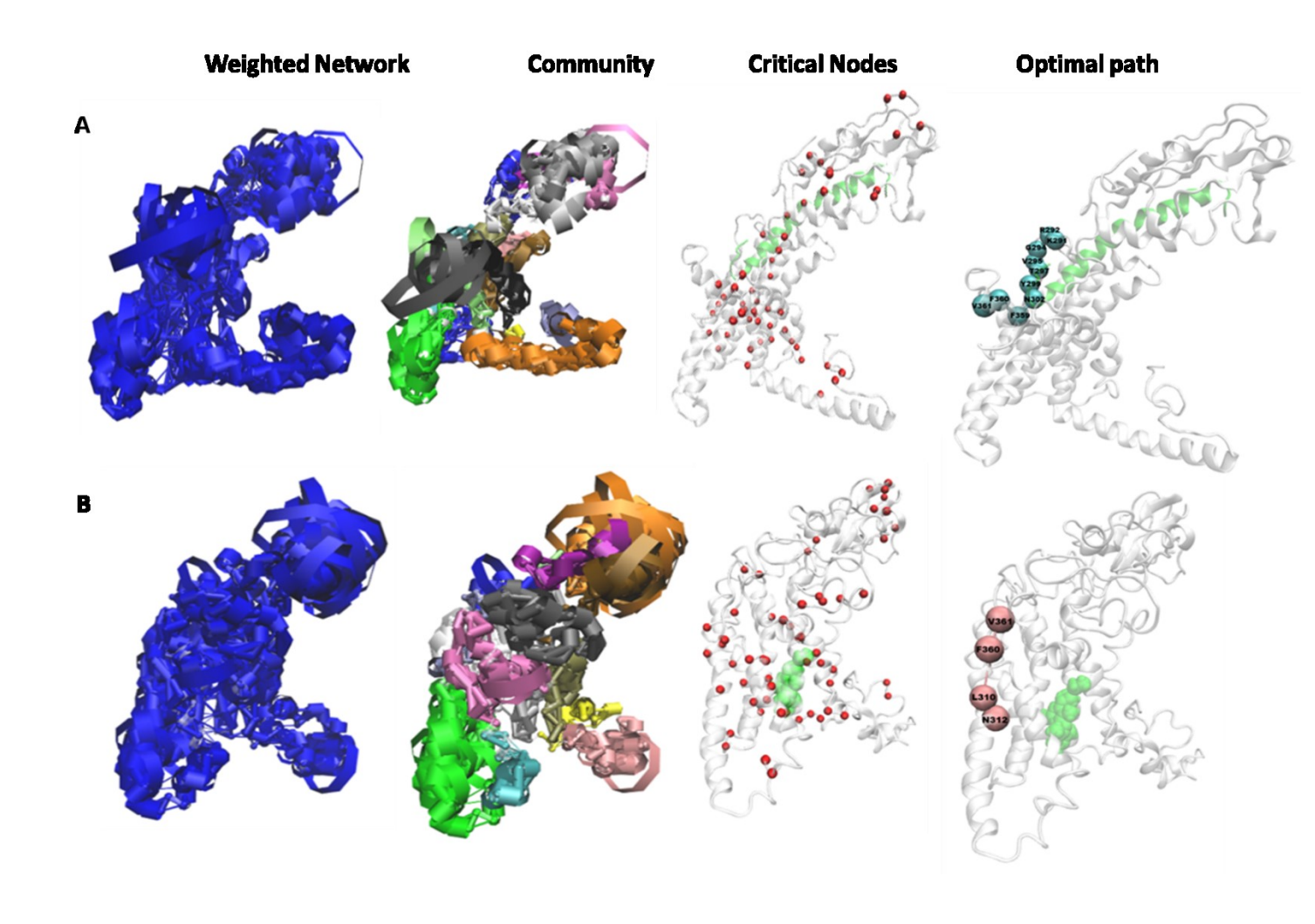


Figure 9. Dynamical network model analysis. Weighted network, community, critical nodes, and possible signal transduction path from ligand binding site to TM6: (**A**) Agonist system and (**B**) Antagonist system. The thickness of the edges reflects the frequency of connection between communities. There are 18 communities in the agonist system and 16 communities in the antagonist system. Possible signal transduction path from ligand binding site to TM6.

Discussion

The lack of high-resolution crystal structures of full-length CRF1R in complex with peptide hormone hinders the design of CRF1R ligand. Studies on the binding of small molecule antagonist ligands to the CRF1R have been performed using the available crystal structure of TMD (PDB ID: 4K5Y) ^{12, 16, 22}. This is the first study with the full-length CRF1R bound to

peptide ligands.CRF1R-selective peptide agonist Urocortin 1 is used to study conformational changes associated with activation. In the constructed complex, the agonists protrude into a groove between TM6 and TM7, pushing them apart as a part of the activation mechanism 9. Following extensive conformational samplings, the peptide agonist-bound CRF1R, relative to the antagonist-bound system, displays higher TM helical content (56% versus 31%), larger RMSD of the TMD (4.5 Å versus 2.7 Å)—in particular, TM6 (8.1 Å versus 5.2 Å), but smaller RMSF (3.6 Å versus 4.3 Å). The Peptide agonist appears to stabilize structures of individual TM helices but induces larger change of their arrangement. These features might be a hallmark of Class B GPCRs. Consistent with a previous study 8, the N-terminal ECD region show clear change of orientation. Activity data suggests that the receptor can still be activated by the peptide agonist upon the removal of N-terminal ECD ²³. Therefore, the TM6 should plays more role in activation. The relative change of the orientation of TM helices, especially TM6, can allow for accommodation of G-protein. For the rearrangement of TM helices to occur, salt bridges and Hbonds are broken at ECL2 and ECL3 and at the intracellular side the TM helices—close to the G-protein binding site. ECL2 is known for contributing to ligand binding in CRF1R ²⁴, and is believed to play a critical role in activation of class B GPCRs ²⁵. This is in line with the strong salt bridge between K291^{ECL2} in CRF1R and D2 in Urocortin 1 (Figure 3A-C). In agreement with these conformational changes, the residue distance between S333^{6.30} and L395^{7.59} increases in the agonist Urocortin 1-bound CRF1R. It is likely that the extracellular motions of TM6 and TM7, caused by the intrusion of Urocortin 1 into the groove between the two helices, get converted into intracellular events (Figure 10). This corroborates with the general belief that a global displacement of TM6 is a key feature of GPCR activation ⁷, thus, suggesting similarity between Class A and Class B GPCRs.

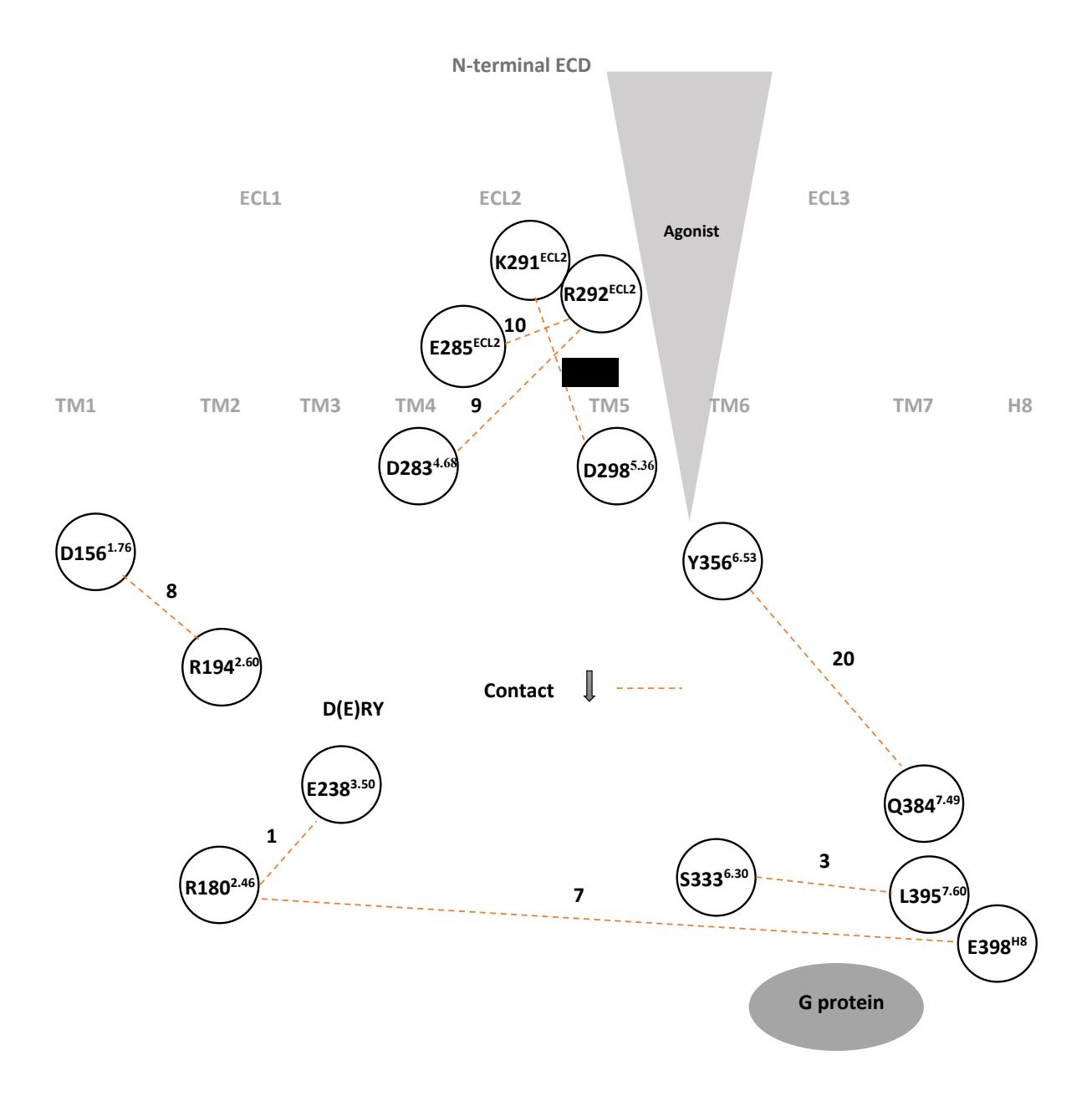


Figure 10. Proposed mechanism of Urocortin 1-induced CRF1R activation. Inter-helical/interregional salt bridges and H-bonds were broken at the peptide binding site within the transmembrane domain (TMD) region and deep inside close to the G-protein binding site. Index number of each residue is assigned based on the list of all the residue distances examined in this

study. Note: R180^{2.46}, H184^{2.50}, E238^{3.50} and Q384^{7.49} are 83% conserved in class B and subfamily B 1 of class B GPCRs. R194^{2.60}, Y356^{6.53}, and E398^{H8} are 66%, 72%, and 83% conserved, respectively, in subfamily B1 of class B GPCRs. Y356^{6.53}, Q384^{7.49}, and L395^{7.60} are critical residues identified by network analysis that overlap with mutagenesis data. K291^{ECL2} is a key interacting residue (Occupancy: >80%) that overlap with mutagenesis data.

In the case of agonist system, the strong connections to TM6 revealed in network analysis indicates its important roles in CRF1R activation. Among 39 critical residues for the agonist Urocortin 1-bound CRF1R, F72, L169^{1.60}, F232^{3.44}, I314^{5.52}, L309^{5.47}, Y356^{6.53}, Q384^{7.49}, and L395^{7.60} overlap with experimental mutagenesis data. Q384^{7.49} is 83% conserved in class B GPCRs; Y356^{6.53} is 66% conserved in subfamily B 1 of class B GPCRs; and L395^{7.60} (not conserved) is the last residue at TM7. These 3 residues are also involved in the 8 inter-residue distances that show increasing trend in the agonist Urocortin 1-bound CRF1R (see Table 2). The optimal path of signal transduction is shorter in the antagonist-CP-376395-bound CRF1R due to the binding of the ligand deep inside the TMD close to TM6 where the signal is thought to be relayed. The signal may be passed from the ECL2 along residues within TM6 to cause the movement of the helix and subsequent activation of the receptor. The simulation data provide insights into the activation of CRF1R by peptide Urocortin 1 which involves large-scale conformational changes leading to the opening of binding space for G-protein—a common hallmark of class B GPCR activation.

Conclusion

To elucidate the activation mechanism of CRF1R, multiple microsecond long MD simulations were carried out on the agonist Urocortin 1-bound CRF1R and antagonist CP-376395-bound CRF1R. The Peptide agonist appears to stabilize the TM helices but induces larger change of their arrangement of helix packing, highlighted by the movement of TM6. Such rearrangement is likely due to the breakage of inter-helical/inter-regional salt-bridges and hydrogen bonds.

Dynamical network analysis reveals the correlation across distant regions for allosteric communications, and communities with frequent connections to TM6. Residues identified from simulation and dynamical network analysis overlap with experimental mutagenesis data. The findings of this work may aid the design ligands targeting CRF1R for treatment of stress-related diseases.

Methods

Homology model generation

The full length sequence of CRF1R comprising 444 amino acids was retrieved from the UniProt database (uniprot ID: P34998) and submitted to I-TASSER online server ²⁶ for model building by "iterative template-based fragment assembly simulation"²⁷. The model selected prioritized PDB structures, 4K5Y ¹⁷ and 3EHU ¹⁸ because the former represents the TMD of inactivated CRF1R, and the latter represents the N-terminal ECD.

Protein and ligand preparation, and docking

Maestro's Protein Preparation Wizard ²⁸ was used to prepare the CRF1R model for MD simulations. Preprocessing was performed on the protein which corrected the bond orders, added hydrogens and disulfide bonds where necessary, assigned correct atom charges based on the protonation state of the titratable residues using predicted pKa values at physiological pH. The charge state was optimized, and restrained minimization was carried out.

Ligand preparation: Three-dimensional (3D) structure of the peptide agonist Urocortin 1 was retrieved from the PBD (PDB ID: 2RMG) complex. The structure of the small molecule

antagonist CP-376395 was extracted from 4K5Y complex and transferred to its orthosteric binding site in the built model.

Docking: Default settings were used under the SP-Peptide mode to dock the prepared peptide ligand using an OPLS3 force field in Glide Docking toolkit available in Schrödinger Suite ²⁹. The docked complex was then loaded on Visual Molecular Dynamics (VMD) software³⁰ for binding pose optimization. The C-terminal end of the peptide ligand was oriented to bind to the ECD in accordance with Grace et al. ^{31,32} who suggest that due to the hydrophobic nature of the region, the C-terminal end expresses receptor specific binding to the ECD.

Molecular dynamics simulation

Molecular dynamics simulation setup

MD simulations were carried out using Desmond ³³. The complexes were aligned in a membrane set to the helices of the 7 transmembrane domain (7TMD), and an OPLS3 force field ³⁴ was employed for system building using the Desmond System Builder toolkit. The two built systems were solvated using a water box with a predefined SPC water model and ionized by addition of 0.15M NaCl.

MD simulation protocols

The default relaxation protocol for membrane proteins ²⁷ was used to relax each system, and this consists of eight steps: 1) Minimization with restraints on solute heavy atoms; 2) Minimization without any restraints; 3) Simulation with heating from 0 K to 300 K, H₂O and gradual restraining; 4) Simulation in NPT (constant number of particles, constant pressure of 1 bar and constant temperature of 300 K) ensemble with H₂O barrier and with heavy atoms restrained; 5) Simulation in NPT ensembles with equilibration of solvent and lipids; 6). Simulation in NPT

ensemble with protein heavy atoms annealing from 10.0 kcal/mol to 2.0 kcal/mol; 7) Simulation in NPT ensemble with Cα atoms restrained at 2 kcal/mol; and 8). Simulation for 1.5 ns in NPT ensemble with no restraints. Finally, three separate 1000 ns production runs with different initial velocity were carried in NPT ensemble for each of the two systems using the default protocol. Temperature was controlled using the Nosé-Hoover chain coupling scheme ³⁵ with a coupling constant of 1.0 ps. Pressure was controlled using the Martyna-Tuckerman-Klein chain coupling scheme ³⁵ with a coupling constant of 2.0 ps. M-SHAKE ³⁶ was applied to constrain all bonds connecting hydrogen atoms, enabling a 2.0 fs time step in the simulations. The k-space Gaussian split Ewald method ³⁷ was used to treat long-range electrostatic interactions under periodic boundary conditions (charge grid spacing of ~ 1.0 Å, and direct sum tolerance of 10^{-9}). The cutoff distance for short-range non-bonded interactions was 10 Å, and the long-range van der Waals interactions was based on a uniform density approximation. To reduce the computation, non-bonded forces were calculated using an r-RESPA integrator ³⁸ where the short range forces were updated every step and the long range forces were updated every three steps. The trajectories were saved at 50.0 ps intervals for analysis.

clustering analysis

The 3 trajectories of each system were merged and the Desmond trajectory tool in maestro was used for trajectory clustering. Backbone RMSD was used as a structural similarity metric and hierarchical clustering with average linkage was applied. The merging distance cutoff was set to 2.5 Å. Structures of the most abundant cluster (those with a frequency of 5% or greater) were saved for further analysis. The representative structures of the most abundant clusters for the agonist and antagonist systems were aligned and superimposed to compare conformational differences.

Interaction and dynamics analysis

The simulation interaction diagram (SID) tool in maestro was used to analyze receptor-ligand-interactions. The following quantities were computed: Root Mean-Square Deviation (RMSD), Root Mean-Square Fluctuation (RMSF), secondary structure changes, and protein-ligand contacts. The RMSD calculation measures the displacement change of atoms for the entire trajectory with respect to the reference frame. The secondary structure changes were monitored through simulations, with focuses on alpha-helices and beta sheets. The simulation also recorded the type and occupancy of each protein-ligand contact. For the agonist Urocortin 1-bound CRF1R, protein contacts were computed using Protein Interaction Analysis toolkit. The resulting data were used to make a table of interactions, and the locations of residues involved were indicated in snake plot representation of CRF1R.

SID analysis calculated the total RMSD for the entire system. For a selected region, all frames were aligned with their respective starting positions based solely on their TMD.

Simulation event analysis toolkit in Maestro was then used to calculate RMSD of each region for the entire trajectory.

Comparison to other GPCRs

The representative structure of the most abundant cluster of each system was aligned with the crystal structure of G-protein-docked Glucagon-like peptide-1 receptor (GLP1-R) (PDB ID 6B3J) ³⁹ based on TMD and then superimposed to observe key conformational changes that may allow for G-protein docking.

Sequence alignment

To identify critical residues for function of CRF1R and the class B GPCR at large, a multiple sequence alignment using "seed-and-extend model" on the protein families database (pfam 33.1)(http://pfam.xfam.org/)⁴⁰ was performed. Conserved residues in class B as well as within subfamily B 1 GPCRs were identified.

Molecular switch and residue distance analysis

Molecular switches are a set of non-covalent interactions that stabilize protein structures. Their formation or breakage is thought to play a role, respectively, in the activation or inactivation of a receptor ¹⁹. Unlike in class A GPCRs, there are no canonical motifs for these microswitches in the class B GPCRs. Therefore, the following potential molecular switches examined by previous studies ^{16, 20} were re-examined in this study: ionic lock between R180^{2.46} and E238^{3.50}; polar lock between H184^{2.50} and E238^{3.50}. Other residue distance examined by the studies cited above were also re-examined. In addition, the gate residue distance between S333^{6.30} and L395^{7.59}, and several inter-helical/inter-regional salt bridges and side chain-side chain hydrogen bonds were examined (Table S5).

Dynamical network analysis

To propose signal transduction pathways leading to activation or inactivation of the receptor respectively by the peptide agonist Urocortin 1, and the small molecule antagonist CP-376395, respectively, NetworkView plugin ⁴¹ in VMD ³⁰ was used to generate a dynamic network model, defined as a set of nodes connected by edges ⁴¹. A contact map was generated for the whole trajectory of each system. Contact map added an edge between nodes whose heavy atoms interacted within a cutoff of 4.5Å for at least 75% of the MD simulation time. Using pairwise

correlations between nodes ⁴¹, the edge distance was derived by the program Carma ⁴². The probability of information transfer across the edge was the computed using the equation bellow:

$$C_{ij} = \frac{\langle \Delta \overrightarrow{r_i}(t) \cdot \Delta \overrightarrow{r_j}(t) \rangle}{(\langle \Delta \overrightarrow{r_i}(t)^2 \rangle \langle \Delta \overrightarrow{r_j}(t)^2 \rangle)^{1/2}}$$

$$\Delta r (t) = ri(t) - \langle ri(t) \rangle$$

Where C_{ij} is the correlation coefficient. The edges are weighted (w_{ij}) between any two nodes i and j: $w_{ij} = -\log(|C_{ij}|)$. Thicker edge denotes a higher probability of information transfer.

Each of the generated networks was then further grouped into subnetworks, referred to as communities, based on groups of nodes with stronger and more frequent connection to each other using Girvan-Newman algorithm ⁴³. The critical nodes that connect communities to one another were identified. An optimal communication path between the ligand binding site and transmission switch was generated.

Supporting Information

- Mean RMSF values of the specific regions of CRF1R for 3 trajectories (1000 ns each).
- Interaction between CRF1R and peptide agonist Urocortin 1 over three trajectories (1000 ns long each).
- Mean values for the complete residue distances examined.
- Mean residue distance examined in the literature, conserved residues (≥ 83%) in class B
 and subfamily B1 GPCRs.
- Residue distance for molecular switches (1-2), gate residue distance between TM6 and TM7 (3), and for remote residues in antagonist binding site (4-6) examined in the literature. Potential interhelical salt bridges (7-17) and side chain-side chain H-bonds (18-21) examined in this study.
- Comparison between our homology model and the crystal structures (PDB 3EHU and 4K5Y).
- RMSD profiles of the individual trajectories and the for the average of the 3 trajectories representative structures of clusters ranked from most abundant to least abundant.
- Evolution of the agonist Urocortin 1-bound CRF1R systems.
- Evolution of the antagonist CP-376395-bound CRF1R.
- The average RMSF profiles of CRF1R and small molecule CP-376395.
- Docked pose of peptide agonist urocortin 1 and small molecule antagonist CP-376395.
- Snake representation of stable interaction; contact between CRF1R and peptide agonist
 Urocortin 1 in the representative of stable interaction between structure of the most abundant cluster.

- Interaction between CRF1R and peptide agonist Urocortin 1 in the representative structure of the most abundant cluster and interaction between CRF1R and the small antagonist CP 376395.
- Unweighted network, communities, and suboptimal paths.
- Multiple sequence alignment of class B GPCRs; multiple sequence alignment of Subfamily B 1 GPCRs of class B GPCRs.
- Critical residues identified via dynamic network analysis overlapping with the conserved residues in class B and subfamily B 1 GPCRs.
- Sequence alignment of agonist Urocortins 1-3, CRF and antagonist Astressin

Acknowledgements

We acknowledge the support to C. W. from the National Science Foundation of USA under grants NSF RUI-1904797/ACI-1429467, XSEDE MCB 170088 and from the Pittsburgh Supercomputing Center and D. E. Shaw Research under a grant MCB170090P. The grants from National Natural Science Foundation of China (11575021, U1930402) to H.L. are also acknowledged

References

- 1. Pal, K.; Melcher, K.; Xu, H. E., Structure and mechanism for recognition of peptide hormones by Class B G-protein-coupled receptors. *Acta Pharmacologica Sinica* **2012**, *33* (3), 300-311.
- 2. Ashton, J. C.; Wright, J. L.; McPartland, J. M.; Tyndall, J. D., Cannabinoid CB1 and CB2 receptor ligand specificity and the development of CB2-selective agonists. *Curr Med Chem* **2008**, *15* (14), 1428-43.
- 3. Alfonso-Prieto, M.; Navarini, L.; Carloni, P., Understanding Ligand Binding to G-Protein Coupled Receptors Using Multiscale Simulations. *Frontiers in Molecular Biosciences* **2019**, *6*.
- 4. Agren, R.; Zeberg, H.; Stepniewski, T. M.; Free, R. B.; Reilly, S. W.; Luedtke, R. R.; Arhem, P.; Ciruela, F.; Sibley, D. R.; Mach, R. H.; Selent, J.; Nilsson, J.; Sahlholm, K., Ligand with Two Modes of Interaction with the Dopamine D2 Receptor-An Induced-Fit Mechanism of Insurmountable Antagonism. *ACS Chem Neurosci* **2020**, *11* (19), 3130-3143.
- 5. Uba, A. I.; Radicella, C.; Readmond, C.; Scorese, N.; Liao, S.; Liu, H.; Wu, C., Binding of agonist WAY-267,464 and antagonist WAY-methylated to oxytocin receptor probed by all-atom molecular dynamics simulations. *Life Sci* **2020**, *252*, 117643.
- 6. Harmar, A. J., Family-B G-protein-coupled receptors. *Genome Biol* **2001**, *2* (12), REVIEWS3013.
- 7. Garelja, M. L.; Au, M.; Brimble, M. A.; Gingell, J. J.; Hendrikse, E. R.; Lovell, A.; Prodan, N.; Sexton, P. M.; Siow, A.; Walker, C. S.; Watkins, H. A.; Williams, G. M.; Wootten, D.; Yang, S. H.; Harris, P. W. R.; Hay, D. L., Molecular Mechanisms of Class B GPCR Activation: Insights from Adrenomedullin Receptors. *ACS Pharmacology & Translational Science* **2020**, *3* (2), 246-262.
- 8. Seidal, L.; Zarzycka, B.; Zaidi, S. A.; Katritch, V.; Coin, I., Structural insight into the activation of a class B G-protein-coupled receptor by peptide hormones in live human cells. *eLife* **2017**, *6*, 25.
- 9. Coin, I.; Katritch, V.; Sun, T.; Xiang, Z.; Siu, Fai Y.; Beyermann, M.; Stevens, Raymond C.; Wang, L., Genetically Encoded Chemical Probes in Cells Reveal the Binding Path of Urocortin-I to CRF Class B GPCR. *Cell* **2013**, *155* (6), 1258-1269.
- 10. Garelja, M. L.; Au, M.; Brimble, M. A.; Gingell, J. J.; Hendrikse, E. R.; Lovell, A.; Prodan, N.; Sexton, P. M.; Siow, A.; Walker, C. S.; Watkins, H. A.; Williams, G. M.; Wootten, D.; Yang, S. H.; Harris, P. W. R.; Hay, D. L., Molecular Mechanisms of Class B GPCR Activation: Insights from Adrenomedullin Receptors. *ACS Pharmacol Transl Sci* **2020**, *3* (2), 246-262.
- 11. Kean, J.; Bortolato, A.; Hollenstein, K.; Marshall, F. H.; Jazayeri, A., Conformational thermostabilisation of corticotropin releasing factor receptor 1. *Sci Rep* **2015**, *5*, 11.
- 12. Teleb, M.; Kuppast, B.; Spyridaki, K.; Liapakis, G.; Fahmy, H., Synthesis of 2-imino and 2-hydrazono thiazolo[4,5-d]pyrimidines as corticotropin releasing factor (CRF) antagonists. *European Journal of Medicinal Chemistry* **2017**, *138* (Supplement C), 900-908.
- Gulyas, J.; Rivier, C.; Perrin, M.; Koerber, S. C.; Sutton, S.; Corrigan, A.; Lahrichi, S. L.; Craig, A.
 G.; Vale, W.; Rivier, J., Potent, structurally constrained agonists and competitive antagonists of corticotropin-releasing factor. *Proceedings of the National Academy of Sciences* 1995, 92 (23), 10575-10579.
- 14. Rivier, J.; Rivier, C.; Vale, W., Synthetic competitive antagonists of corticotropin-releasing factor: effect on ACTH secretion in the rat. *Science* **1984**, *224* (4651), 889-891.
- 15. Brauner-Osborne, H.; Wellendorph, P.; Jensen, A. A., Structure, pharmacology and therapeutic prospects of family C G-protein coupled receptors. *Curr Drug Targets* **2007**, *8* (1), 169-84.
- 16. Xu, J. L.; Wang, Z. H.; Liu, P.; Li, D. M.; Lin, J. P., An insight into antagonist binding and induced conformational dynamics of class B GPCR corticotropin-releasing factor receptor 1. *Mol. Biosyst.* **2015**, *11* (7), 2042-2050.

- 17. Hollenstein, K.; Kean, J.; Bortolato, A.; Cheng, R. K.; Dore, A. S.; Jazayeri, A.; Cooke, R. M.; Weir, M.; Marshall, F. H., Structure of class B GPCR corticotropin-releasing factor receptor 1. *Nature* **2013**, *499* (7459), 438-43.
- 18. Pioszak, A. A.; Parker, N. R.; Suino-Powell, K.; Xu, H. E., Molecular recognition of corticotropin-releasing factor by its G-protein-coupled receptor CRFR1. *J Biol Chem* **2008**, *283* (47), 32900-12.
- 19. Kobilka, B. K.; Deupi, X., Conformational complexity of G-protein-coupled receptors. *Trends Pharmacol. Sci.* **2007**, *28* (8), 397-406.
- 20. Sun, X.; Cheng, J.; Wang, X.; Tang, Y.; Ågren, H.; Tu, Y., Residues remote from the binding pocket control the antagonist selectivity towards the corticotropin-releasing factor receptor-1. *Sci Rep* **2015**, *5* (1).
- 21. Mishra, S. K.; Jernigan, R. L., Protein dynamic communities from elastic network models align closely to the communities defined by molecular dynamics. *PLoS One* **2018**, *13* (6), e0199225.
- 22. Dunlop, B. W.; Binder, E. B.; Iosifescu, D.; Mathew, S. J.; Neylan, T. C.; Pape, J. C.; Carrillo-Roa, T.; Green, C.; Kinkead, B.; Grigoriadis, D.; Rothbaum, B. O.; Nemeroff, C. B.; Mayberg, H. S., Corticotropin-Releasing Factor Receptor 1 Antagonism Is Ineffective for Women With Posttraumatic Stress Disorder. *Biol. Psychiatry* **2017**, *82* (12), 866-874.
- 23. Zhao, L. H.; Yin, Y.; Yang, D.; Liu, B.; Hou, L.; Wang, X.; Pal, K.; Jiang, Y.; Feng, Y.; Cai, X.; Dai, A.; Liu, M.; Wang, M. W.; Melcher, K.; Xu, H. E., Differential Requirement of the Extracellular Domain in Activation of Class B G Protein-coupled Receptors. *J Biol Chem* **2016**, *291* (29), 15119-30.
- 24. Assil-Kishawi, I.; Abou-Samra, A. B., Sauvagine cross-links to the second extracellular loop of the corticotropin-releasing factor type 1 receptor. *J Biol Chem* **2002**, *277* (36), 32558-61.
- 25. Koole, C.; Wootten, D.; Simms, J.; Miller, L. J.; Christopoulos, A.; Sexton, P. M., Second extracellular loop of human glucagon-like peptide-1 receptor (GLP-1R) has a critical role in GLP-1 peptide binding and receptor activation. *J Biol Chem* **2012**, *287* (6), 3642-58.
- 26. Zhang, Y., I-TASSER server for protein 3D structure prediction. *Bmc Bioinformatics* **2008**, *9*.
- 27. Zhang, J.; Hou, Y.; Wang, Y.; Wang, C.; Zhang, X., The LBFGS quasi-Newtonian method for molecular modeling prion AGAAAAGA amyloid fibrils. *Natural Science* **2012**, *04* (12), 1097-1108.
- 28. Sastry, G. M.; Adzhigirey, M.; Day, T.; Annabhimoju, R.; Sherman, W., Protein and ligand preparation: parameters, protocols, and influence on virtual screening enrichments. *Journal of computer-aided molecular design* **2013**, *27* (3), 221-34.
- 29. Friesner, R. A.; Banks, J. L.; Murphy, R. B.; Halgren, T. A.; Klicic, J. J.; Mainz, D. T.; Repasky, M. P.; Knoll, E. H.; Shelley, M.; Perry, J. K.; Shaw, D. E.; Francis, P.; Shenkin, P. S., Glide: a new approach for rapid, accurate docking and scoring. 1. Method and assessment of docking accuracy. *J Med Chem* **2004**, *47* (7), 1739-49.
- 30. Humphrey, W.; Dalke, A.; Schulten, K., VMD: Visual molecular dynamics. *Journal of Molecular Graphics* **1996**, *14* (1), 33-38.
- 31. Grace, C. R.; Perrin, M. H.; Cantle, J. P.; Vale, W. W.; Rivier, J. E.; Riek, R., Common and divergent structural features of a series of corticotropin releasing factor-related peptides. *Journal of the American Chemical Society* **2007**, *129* (51), 16102-14.
- 32. Grace, C. R.; Perrin, M. H.; Gulyas, J.; Digruccio, M. R.; Cantle, J. P.; Rivier, J. E.; Vale, W. W.; Riek, R., Structure of the N-terminal domain of a type B1 G protein-coupled receptor in complex with a peptide ligand. *Proceedings of the National Academy of Sciences of the United States of America* **2007**, *104* (12), 4858-63.
- 33. Bowers, K. J.; Chow, D. E.; Xu, H.; Dror, R. O.; Eastwood, M. P.; Gregersen, B. A.; Klepeis, J. L.; Kolossvary, I.; Moraes, M. A.; Sacerdoti, F. D.; Salmon, J. K.; Shan, Y.; Shaw, D. E., Scalable Algorithms for Molecular Dynamics Simulations on Commodity Clusters. In *ACM/IEEE SC 2006 Conference (SC'06)*, 2006; pp 43-43.

- 34. Harder, E.; Damm, W.; Maple, J.; Wu, C.; Reboul, M.; Xiang, J. Y.; Wang, L.; Lupyan, D.; Dahlgren, M. K.; Knight, J. L.; Kaus, J. W.; Cerutti, D. S.; Krilov, G.; Jorgensen, W. L.; Abel, R.; Friesner, R. A., OPLS3: A Force Field Providing Broad Coverage of Drug-like Small Molecules and Proteins. *J Chem Theory Comput* **2016**, *12* (1), 281-96.
- 35. Ikeguchi, M., Partial rigid-body dynamics in NPT, NPAT and NP gamma T ensembles for proteins and membranes. *Journal of Computational Chemistry* **2004**, *25* (4), 529-541.
- 36. Bailey, A. G.; Lowe, C. P., MILCH SHAKE: An Efficient Method for Constraint Dynamics Applied to Alkanes. *Journal of Computational Chemistry* **2009**, *30* (15), 2485-2493.
- 37. Shan, Y. B.; Klepeis, J. L.; Eastwood, M. P.; Dror, R. O.; Shaw, D. E., Gaussian split Ewald: A fast Ewald mesh method for molecular simulation. *Journal of Chemical Physics* **2005**, *122* (5).
- 38. Stuart, S. J.; Zhou, R. H.; Berne, B. J., Molecular dynamics with multiple time scales: The selection of efficient reference system propagators. *Journal of Chemical Physics* **1996**, *105* (4), 1426-1436.
- 39. Liang, Y. L.; Khoshouei, M.; Glukhova, A.; Furness, S. G. B.; Zhao, P.; Clydesdale, L.; Koole, C.; Truong, T. T.; Thal, D. M.; Lei, S.; Radjainia, M.; Danev, R.; Baumeister, W.; Wang, M. W.; Miller, L. J.; Christopoulos, A.; Sexton, P. M.; Wootten, D., Phase-plate cryo-EM structure of a biased agonist-bound human GLP-1 receptor-Gs complex. *Nature* **2018**, *555* (7694), 121-125.
- 40. El-Gebali, S.; Mistry, J.; Bateman, A.; Eddy, S. R.; Luciani, A.; Potter, S. C.; Qureshi, M.; Richardson, L. J.; Salazar, G. A.; Smart, A.; Sonnhammer, E. L. L.; Hirsh, L.; Paladin, L.; Piovesan, D.; Tosatto, S. C. E.; Finn, R. D., The Pfam protein families database in 2019. *Nucleic Acids Res* 2019, 47 (D1), D427-D432.
- 41. Eargle, J.; Luthey-Schulten, Z., NetworkView: 3D display and analysis of protein·RNA interaction networks. *Bioinformatics* **2012**, *28* (22), 3000-3001.
- 42. Glykos, N. M., Software news and updates. Carma: a molecular dynamics analysis program. *J Comput Chem* **2006**, *27* (14), 1765-8.
- 43. Girvan, M.; Newman, M. E. J., Community structure in social and biological networks. *Proceedings of the National Academy of Sciences* **2002**, *99* (12), 7821.